Modified Oxymethylene Ethers Based on Technical Alcohol Mixtures and their Fuel Properties

Victor Zaghini Francesconi, Marius Drexler, Thomas A. Zevaco, Ulrich Arnold* and Jörg Sauer

DOI: 10.1002/cite.202400159

Supporting Information available online

Oxymethylene dimethyl ethers (OMDME) have attracted interest as renewably synthesized diesel substitutes with low soot formation and NO_x emissions. In order to enable a high compatibility of this new type of fuel in the already existing infrastructure, a modified oxymethylene ether (OME) synthesis based on technical alcohol mixtures, i.e., C_4-based alcohol mixtures of isomers, was evaluated and the new compounds were thoroughly characterized. The synthesized compounds can be used as neat fuel or as blending component for fossil or paraffinic diesel fuels. The modification of OME offers the possibility to adjust desired properties. This versatility could also be used to synthesize compounds for the chemical sector according to its respective requirements, such as applications as solvents, plasticizers, or additives.

Keywords: Diesel fuels, Fuel blends, Heterogeneous catalysis, Oxymethylene ethers, Synthetic fuels

Received: November 29, 2024; *revised:* December 20, 2024; *accepted:* January 08, 2025

1 Introduction

Concerning future sustainable mobility, several hard-to-electrify applications in the transportation sector and machinery usage, e.g., heavy duty off-road applications, still require the use of dense liquid fuels [1–4]. In 2019, the global transportation sector was the fourth largest source of greenhouse gas emissions and made up roughly 15 % of total greenhouse gas emissions [4]. These emissions averaged a 1.8 % annual growth since 2010, and road transport for passengers and freight is the largest source of transport emissions, making up over two-thirds of the sector's total [4]. Hence, the transport sector is heavily reliant on combustion engines and therefore on liquid fuels. More than 50 % of the global transport energy demand is encompassed by heavy duty, marine, and air transport [2, 3].

A complete exchange of internal combustion engine vehicles by electric battery systems would be particularly challenging, as it would require large capacities for generation, storage, and distribution of renewable electric power. Therefore, the efficient production of renewable energy carriers, e.g., as alternative diesel fuels in the heavy duty sector, still represents a major challenge and necessity to keep the current infrastructure working and at the same time reduce emissions. In this context, oxygenates, especially oxymethylene ethers (OME), more specifically, oxymethylene dimethyl ethers (OMDME), have attracted interest as renewably synthesized diesel substitutes [5–14]. OMDME are linear acetals with the formula $CH_3O(CH_2O)_nCH_3$. Due to the lack of C—C bonds, virtually no soot formation is measured during combustion, resolving the soot-NO_x trade-off.

In general, OME synthesis is an acid-catalyzed reaction, which can be carried out under mild conditions in terms of temperature and pressure. Based on a source of formaldehyde and methanol or its derivatives, various studies elaborate on the continuous production of OMDME [15]. OMDME synthesis from methanol and formaldehyde is illustrated in Fig. 1.

[1]Victor Zaghini Francesconi, [1]Marius Drexler,
[1]Dr. Thomas A. Zevaco,
[1]Dr. Ulrich Arnold (ulrich.arnold@kit.edu), [1]Prof. Jörg Sauer
[1]Karlsruhe Institute of Technology (KIT), Institute of Catalysis Research and Technology (IKFT), Hermann-von-Helmholtz-Platz 1, 76344 Eggenstein-Leopoldshafen, Germany.

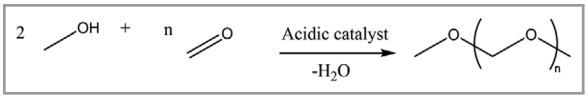

Figure 1. OME synthesis from methanol and formaldehyde.

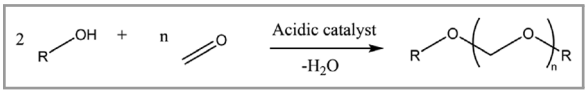

Figure 2. Generalization of OME synthesis employing an alcohol R–OH and formaldehyde, with R representing an alkyl chain other than a methyl end group (–CH_3).

Especially the oligomers with a chain length of $n = 3$–5 are largely compliant with current diesel standards [16]. However, individual properties differ, particularly energy density, cold-stability, and compatibility with currently used elastomeric sealing materials, complicating their use as a neat fuel. Recent studies have shown that a content of 10–20 % OMDME as a blending component with fossil diesel fuel is already sufficient for a significant reduction in soot emissions [10, 12, 13, 17–21]. Hence, a blending strategy with diesel fuels would circumvent the compatibility issues with current engine technology, enabling a simplified and faster application. Furthermore, the miscibility of OMDME with paraffinic diesel fuels (e.g., hydrogenated vegetable oils, HVO) was proven to be challenging [22–28]. To enhance fuel properties, OME can be molecularly modified by introducing new end groups [5, 29–36]. In recent studies, alcohols other than methanol (see Fig. 2) were used in the production process in order to achieve better compatibility with the diesel standard and the existing infrastructure [29–35].

Such modified OME or oxymethylene dialkyl ethers (OMDAE) based on different alcohols (e.g., butanol) or their respective acetal (e.g., butylal) incorporate longer-chain alkyl end groups. These new compounds are of interest for the fuel industry, since they feature more advantageous properties when compared to the methanol-based OMDME. Due to a reduced polarity in the modified OME molecule, an enhancement of the compatibility with sealing materials [32] and miscibility with paraffinic diesel fuels, such as HVO, is possible [23]. Also, the introduction of long, branched end groups was proven to be advantageous, particularly with regard to cold-stability [35]. Thus, the use of different alcohols other than methanol in the production process leads to compounds with advantages regarding important physicochemical properties for the combustion process, such as heating value, density, and cold-stability, as well as higher compatibility with sealing materials and better miscibility with paraffinic diesel [23, 29–35].

Since integration of the OMDAE synthesis into the OME production process is expected to result in the occurrence of asymmetric transacetalization products, dimethoxymethane ($OMDME_1$, DMM) is also used as a starting material. Transacetalization reactions [35–37] occur between two acetals in the presence of an acidic catalyst, as demonstrated in Fig. 3. As described by Haltenort et al. [36] and Voggenreiter et al. [38], when equimolar amounts of substances of the acetals are employed, chemical equilibrium for the transacetalization reaction is achieved when the product composition amounts to 25 mol. % of each starting acetal and 50 mol. % of the corresponding asymmetrical acetal.

Within this work, five different OMDAE were synthesized based on technical alcohols (mixtures of different isomers) and the products were characterized thoroughly. Technical alcohol mixtures, i.e., isoamyl alcohol (IAA) and isononyl alcohol (INA), as well as DMM were used, as indicated in Fig. 4. IAA and INA are mixtures of isomers, as described by the manufacturers. IAA is a mixture of 2-methylbutan-1-ol and 3-methylbutan-1-ol and INA is a heterogeneous mixture of different C_9 isomers due to the production process. The employed alcohols are based on butene (C_4) [39, 40], which can be synthesized renewably, e.g., by methanol-to-olefins (MTO) or dimethyl ether-to-olefins (DTO) processes [41], as well as via fermentation and biomass conversion processes [42]. By means of hydroformylation, a typical reaction between alkenes and syngas, aldehydes can be produced [43]. The hydrogenation of aldehydes opens a way to alcohols [43], as summarized in Fig. 4. Evonik Oxeno GmbH & Co. KG have a 450 kt/a production for INA, showcasing an existing industrial production of such oxo-alcohols [40]. By employing different well available alcohols as starting materials, specific modification of the end group of OME by branching was achieved and the resulting implications for the physical and fuel properties were evaluated.

2 Experimental

2.1 Materials

Isoamyl alcohol (IAA, mixture of isomers) was obtained from Merck, isononyl alcohol (INA, mixture of isomers) from Evonik Operations GmbH, DMM (>99.7 %) from INEOS Paraform GmbH & Co. KG, trioxane from Merck KgaA, and benzene D6 (deuteration grade 99.8 %) was from

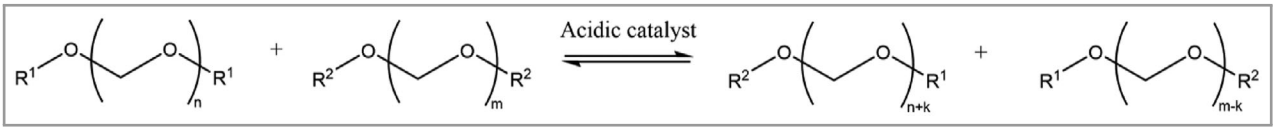

Figure 3. General reaction scheme for transacetalization reactions between acetals in the presence of an acidic catalyst [36].

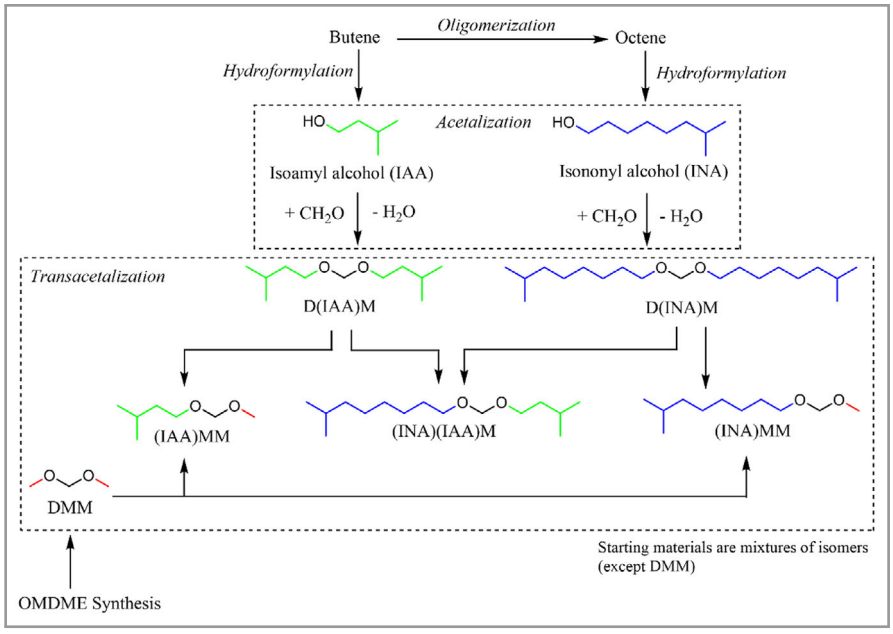

Figure 4. Overview of reactants, reactions, and products of the modified OME synthesis studied in this work.

Sigma-Aldrich. The Amberlyst 36 catalyst was purchased from Sigma-Aldrich and the BEA(25) catalyst from Zeolyst International. Activated carbon powder (0.5–0.75 mm, 20–35 mesh ASTM) and the ion-exchange resin III (strong alkaline ion exchange resin) were bought from Merck KGaA. $OMDME_{3\text{-}5}$ and HVO were obtained from ASG Analytik-Service AG and calcium hydride from Sigma-Aldrich (reagent grade, 95 %).

The zeolite BEA(25) was calcined at 500 °C for 5 h in static air to obtain the active H-form of the catalyst. In order to avoid inhibition of catalytic activity by water [44, 45], all employed catalysts were dried at 110 °C and 10 mbar overnight prior to use. Tab. 1 gives an overview of the employed catalytic materials in this study.

2.2 Synthesis of the Compounds

All experiments were carried out in a 2-L glass flask sealed with a septum and combined with a Dean-Stark apparatus and reflux condenser. The catalyst was contained in a stainless-steel basket, placed in the middle of the flask, and equimolar amounts of the educts were used. An oil bath was employed for heating and the reaction mixtures were stirred magnetically at 500 rpm. The reactions were monitored by continuous sampling. After the reaction, the mixtures were cooled down to room temperature and filtrated.

As alcohols are used for the acetalization step, water is formed during the reaction (see Fig. 2). Since zeolites are known for loss of activity in the presence of water [44, 45], the acetalization was performed with an ion-exchange resin. The acetalization reactions were carried out following the procedure described by Fischer and Giebe [48] at a temperature of 120 °C and 0.3 wt % of catalyst loading (Amberlyst 36). Here, the alcohols (either IAA or INA) were allowed to react with trioxane until stagnation of educt conversion and constant product composition, measured by GC-FID. By employing ion-exchange resins in the acetalization reactions, the possibility of desulfonation and therefore leaching of active sites is possible [49–51]. Thus, in order to ensure that no further reactivity was present, the raw product mixture was neutralized with a strong alkaline ion-exchange resin and treated with activated carbon powder over night at room temperature. Afterwards, the mixture was filtrated over night again and purified by distillation until purity was above 99 % in regard to GC-area of the acetal with a chain length of 1.

The transacetalization reactions were performed in a water-free process at 45 °C and 0.75 wt % of catalyst loading (BEA(25)). The reaction mixtures were prepared starting from equimolar amounts of the acetals. The synthesized acetals were allowed to react with DMM until a constant product composition was measured by GC-FID (at least 72 h). Here, it was assumed that chemical equilibrium was achieved, since 50 mol. % of each initial acetal was converted to the corresponding asymmetrical acetal, as expected and described by Haltenort et al. [36] and Voggenreiter et al. [38]. Another transacetalization reaction was performed employing the acetals from IAA and INA, thus enabling the

Table 1. Summary of relevant characteristics of employed catalysts.

Catalyst	Acidity [mmol g^{-1}]	Surface area [m^2g^{-1}]	Pore volume [cm^3g^{-1}]	Pore diameter [Å]
Amberlyst36	5.4[a)]	33[a)]	0.20[a)]	240[a)]
BEA(25)	0.47 (Brønsted sites)[b)]	680[a)]	0.138 (micro)[b)]; 0.665 (meso)[b)]	6.6 × 6.7; 5.6 × 5.6[c)]

a) Manufacturer's data; b) value from Drexler et al. [46]; c) value from Baerlocher et al. [47].

Table 2. Overview of synthesized compounds and the respective labeling used throughout this work (sorted by increasing molar mass).

Compound	Label	Chemical formula	Molar mass [g mol^{-1}]	Oxygen content [wt %]
(Isopentoxy)methoxymethane	(IAA)MM	$C_7H_{16}O_2$	132.12	24.22
Di(isopentoxy)methane	D(IAA)M	$C_{11}H_{24}O_2$	188.31	16.99
(Isononoxy)methoxymethane	(INA)MM	$C_{11}H_{24}O_2$	188.31	16.99
(Isononoxy)(isopentoxy)methane	(INA)(IAA)M	$C_{15}H_{32}O_2$	244.42	13.09
Di(isononoxy)methane	D(INA)M	$C_{19}H_{40}O_2$	300.53	10.65

synthesis of an asymmetric transacetal with an isoamyl and an isononyl branch in the molecule. An overview of the reaction system is depicted in Fig. 4.

2.3 Analytical Methods

For the analysis of the liquid samples, a Hewlett Packard 6890N series gas chromatograph (GC) coupled with a flame ionization detector (FID) equipped with an Agilent DB-5 MS + DG column (length: 30 m, diameter: 0.25 mm, film: 0.25 µm) was used. The carrier gas was helium.

^{1}H, ^{13}C, and 2D-NMR measurements were recorded under ambient conditions using a Jeol JNM-ECZR series spectrometer equipped with a 9.4 T Oxford cryomagnet (resonance: ^{1}H @399.905 MHz and ^{13}C @100.556 MHz). The spectra were recorded by using benzene D6 (deuteration grade 99.8 %) solutions with a Jeol Royal 5 mm probe head (combination of broadband and inverse detection probe head). The NMR measurements were carried out using the Jeol software Delta 5.3.3. and the standard Jeol pulse sequences, optimizing them if necessary. The NMR spectra are evaluated using MNova 10 (Version 14.2.1-27684). The measurements were conducted by means of the proprietary software of Jeol Delta 5.3.3, the pulse sequences used belong to the standard Delta library and were optimized when necessary. The evaluation and plotting of the spectra were performed with Delta 5.3.3 and the MNova 10 NMR software package.

Mass spectra of the samples were recorded with an Agilent 5973 Network Mass Selective Detector mass spectrometer coupled with an Agilent 6890N GC system. The GC used was equipped with a Restek RTX-5MS column (length: 30 m, diameter: 0.32 mm, film: 0.25 µm). The carrier gas was helium. Mass spectra were evaluated using the software MassHunter Qualitative Analysis from Agilent (Version 10.0).

Density (DIN EN ISO 12185: 1997), kinematic viscosity (DIN EN 16896: 2017), flash point FP (ASTM D7094: 2016), cetane number (DIN EN 17155: 2018), cold filter plugging point CFPP (DIN EN 116: 2018), cloud point CP (DIN EN 23015: 1994), lubricity HFRR (DIN EN ISO 12156-1: 2019), and distillation progress (DIN EN 17306: 2019) of the purified compounds were determined according to the respective standard test methods performed by the certified company ASG Analytik-Service AG. In addition, the higher heating value (HHV) was measured employing a C5003 calorimeter from IKA, with a C5001 cooling system, calibrated with benzoic acid under standard conditions (in-house analytics, maximum relative deviation at ±0.17 %).

3 Results and Discussion

3.1 Characterization of the Synthesized Compounds

The characterization of the synthesized compounds includes NMR spectroscopy, GC-MS, and analysis of relevant physicochemical and fuel properties. The synthesized compounds in this work are listed in Tab. 2. An overview of the synthesis is shown in Fig. 4.

In principle, using different complementary NMR methods allows to clearly identify the structure of new synthesized compounds, provided that their purity is high enough. Generally, the assignment of the numerous NMR signals is made correlating the information gained from 1D methods (e.g., standard ^{1}H and ^{13}C measured using a DEPT135 pulse sequence) and from correlated 2D-NMR spectra, in this case HSQC (heteronuclear single quantum coherence), which can easily determine the proton-carbon connectivity. As an example, typical 1D ^{1}H and ^{13}C spectra together with a 2D ^{13}C, ^{1}H-correlated spectrum are displayed for the acetal of IAA, namely, D(IAA)M (see Tab. 2 for nomenclature). The spectra are presented in Figs. 5–7. However, since the starting materials used in this work are mixtures of isomers, the interpretation of the NMR spectra is equivocal, especially for the isononyl alcohol acetals and transacetals. The complete characterization of the other compounds can be found in the Supporting Information.

The exemplary ^{1}H NMR spectrum of D(IAA)M, a symmetrical molecule, is relatively easy to apprehend, as depicted in Fig. 5 with chemical shift regions and integrations attributed to the related molecule segments. The methyl groups of the isopropyl fragment (fragment 1) can be found around 0.75 ppm. The complementary CH group of the isopropyl group (fragment 2) is detected at 1.63 ppm, showing a typical septet structure due to the two neighboring methyl groups. Fragment 3 (around 1.38 ppm) can be classically attributed to methylene groups belonging to the bulk of an alkane chain. Fragment 4 (low field shifted, around 3.5 ppm) typically represents a methylene group in alpha position relative to an oxygen atom, in our case to the oxymethylene ether group. It is generally displayed as a triplet or a multiplet depending on the length of

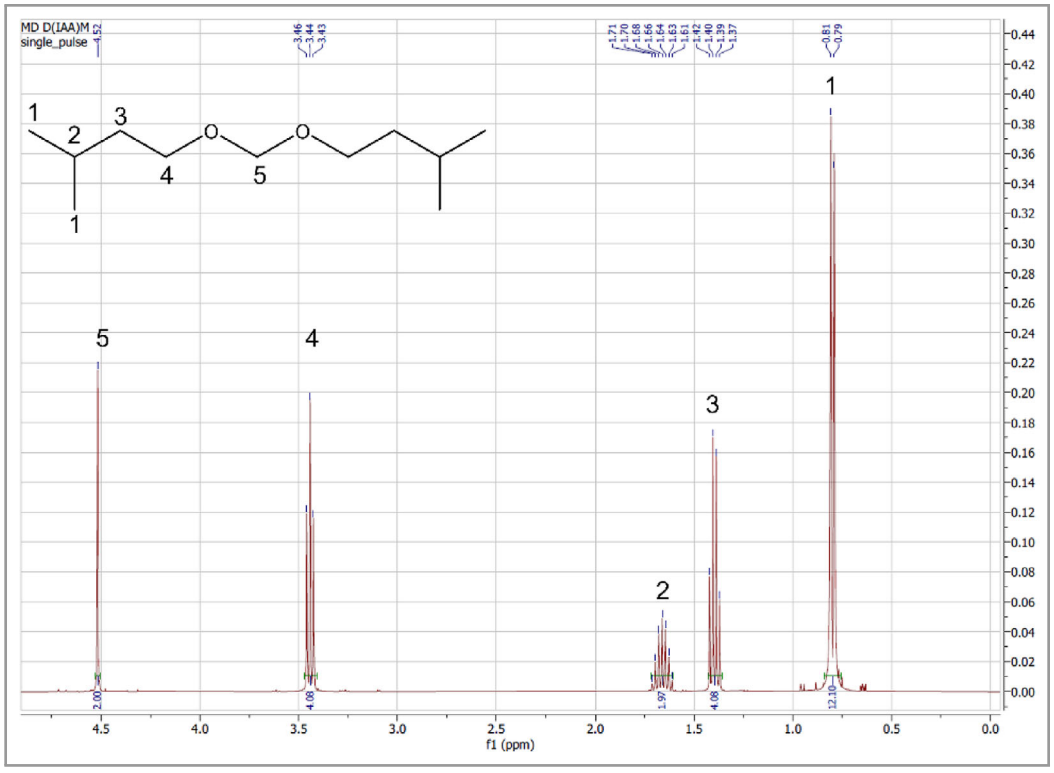

Figure 5. ^{1}H NMR spectrum of D(IAA)M: chemical shift δ in ppm (measured in benzene-d6).

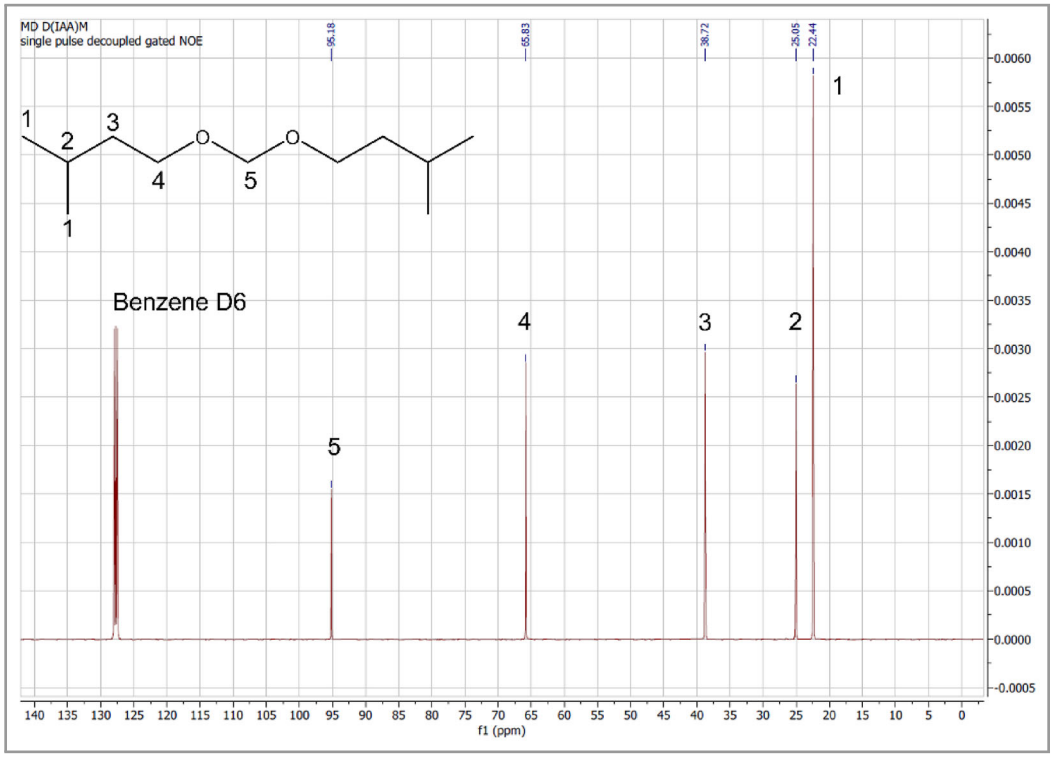

Figure 6. ^{13}C NMR spectrum of D(IAA)M: chemical shift δ in ppm (measured in benzene-d6).

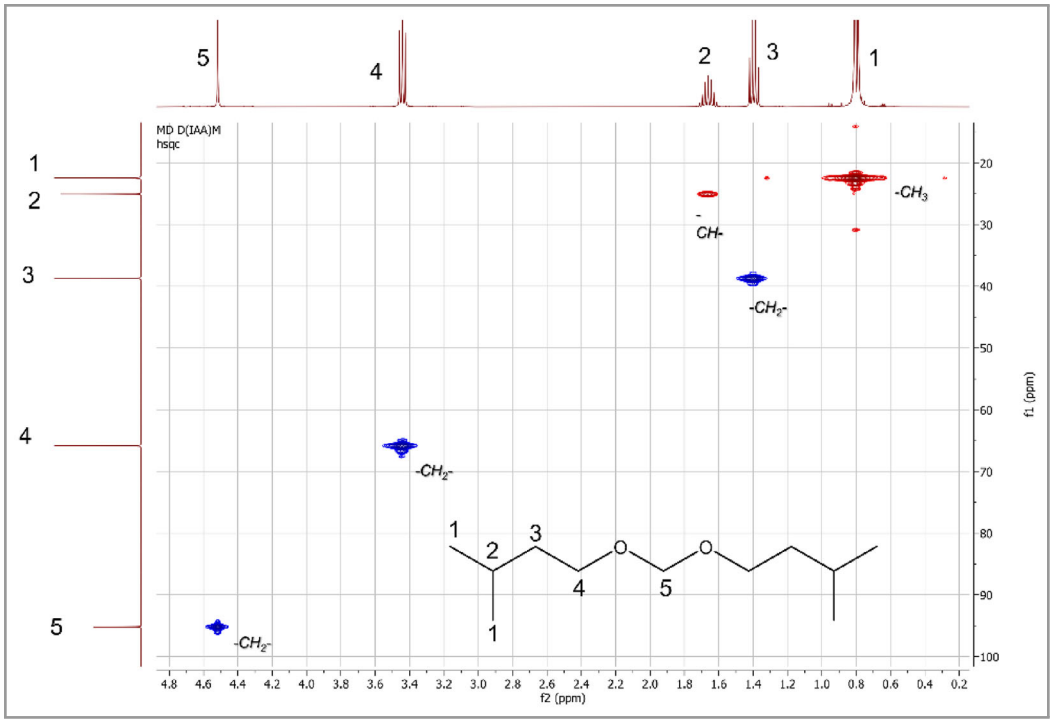

Figure 7. ^{1}H, ^{13}C-HSQC 2D NMR spectrum of D(IAA)M: chemical shift δ in ppm (measured in benzene-d6).

the chain and on the complexity of the coupling patterns within this chain. The clear-cut singulet displayed at lowest field, around 4.5 ppm, is typical for the central methylene group of the acetal substance class (fragment 5), shielded by two oxygen atoms and displaying no interactions (coupling patterns) with the other protons of the alkyl chains.

Analogous to the ^{1}H NMR, the ^{13}C NMR spectrum can be divided into similar chemical shift regions (see Fig. 6). The "pure" alkyl fragments of the molecule can be seen between 15 and 40 ppm. For instance, the carbon of the CH group (fragment 2) has a chemical shift around 25 ppm. Fragment 3 (around 40 ppm) represents the methylene group belonging to the bulk of the alkane chain whereas fragment 4 (around 65 ppm) can be attributed to the methylene group in alpha position of the oxymethylene ether group. The central methylene bridge in fragment 5, typical for the acetal substance class, can be seen at around 95 ppm.

Fig. 7 nicely demonstrates the ability of the 2D HSQC method to easily connect ^{1}H and ^{13}C information and so to rapidly assess the structure of the molecule (^{13}C signals are shown along the f1 (Y) axis, whereas ^{1}H signals are depicted along the f2 (X) axis). Depending on the phase of the signals, it is possible to discern the multiplicity of the carbon, i.e., to discern CH and CH_3 groups from CH_2 groups. With the analysis of these three "basic" spectra (^{1}H, ^{13}C, and ^{1}H, ^{13}C-HSQC) it is possible to systematize the attribution of the different NMR signals to the related molecule fragments and so to rapidly evaluate the success of the synthesis via NMR spectroscopy.

The mass spectrum of the compound D(IAA)M and the most common fragments are presented in Fig. 8. Spectra from the other synthesized substances can be seen in the Supporting Information. Analogously to the NMR spectra, the starting materials used in this work are mixtures of isomers, therefore the interpretation of the GC-MS spectra is equivocal, especially for the isononyl alcohol acetals and transacetals.

The fragmentation of the oxymethylene ether bridge occurs most frequently, with the fragment $C_6H_{13}O^{\bullet}$ having the highest abundancy. A fragmentation generating the species $C_5H_{11}^{\bullet}$ ($m/z = 71.1$) and $C_6H_{13}O_2^{\bullet}$ ($m/z = 117.1$) as well as the species $C_3H_7^{\bullet}$ ($m/z = 43.1$) corresponds well to the data seen in the mass spectrum. The fragment $C_8H_{17}O_2^{\bullet}$ ($m/z = 145.1$) is virtually not seen, therefore it is most likely that this fragment experiences further fragmentation. For instance, the fragment with $m/z = 29.1$ is generally seen by the fragmentation of compounds with formaldehyde building blocks which would imply a possible further fragmentation of the fragment $C_8H_{17}O_2^{\bullet}$ ($m/z = 145.1$). In this case, it is also possible to detect the mass peak ion at $m/z = 187.2$, one unit short of the molar mass of the whole molecule due to ionization.

3.2 Physicochemical and Fuel Properties

To put the properties of the new substances (summarized as OMDAE) into perspective, a comparison with

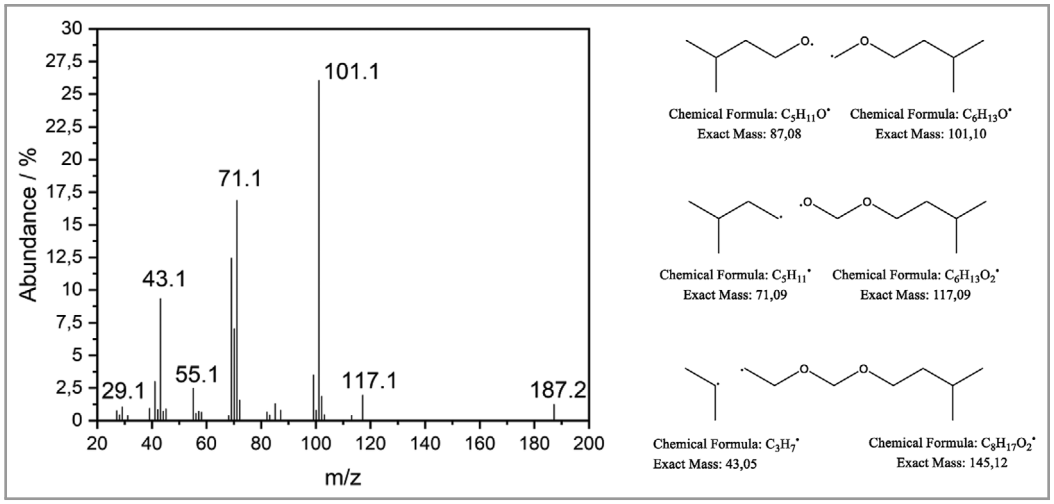

Figure 8. Assignment of relevant fragments of the mass spectrum of D(IAA)M.

Table 3. Overview of physicochemical and fuel properties of the synthesized OMDAE.

Compound	Density at 15 °C [kg m^{-3}]	Kinematic viscosity at 40 °C [mm^{2}s^{-1}]	HFRR [µm]	Cetane number [–]	Flash point [°C]	Cloud point [°C]	CFPP [°C]	HHV [MJ kg^{-1}]
(IAA)MM	843.0	0.769	540	51.4	30.0	<−90	<−61	34.19
D(IAA)M	835.7	1.323	650	68.2	76.5	<−100	−75	38.03
(INA)MM	857.0	1.531	510	79.1	83.5	−103.7	<−61	38.09
(INA)(IAA)M	845.8	2.446	510	76.6	123.0	−46.0	−55	40.17
D(INA)M	854.2	4.290	430	86.5	153.5	<−100	−37	41.21
Diesel (EN 590)	820–845	2.0–4.5	<460	>51	>55	<−7[a]; < 5[b]	<−20[a]; <0[b]	–

a) Winter diesel; b) summer diesel.

methanol-based OMDME with chain length n = 1–5 and with n-alkanes with similar molar mass is made. Properties of all considered compounds can be found in the Supporting Information. Thus, the influence of the molecular structure on different properties can be elucidated. An overview of measured physicochemical and fuel properties of the synthesized compounds is presented in Tabs. 3 and 4, as well as the limits for standard diesel fuels according to specification EN 590. In Tab. 4, the distillation progress and not boiling point is given, since compounds are mixtures of isomers. For comparison of boiling characteristics with OMDME and n-alkanes, the distillation progress at 50 % is used. The distillation range of diesel lies at approximately 180–360 °C (EN 590).

Table 4. Overview of the distillation progress of the synthesized OMDAE, measured at atmospheric pressure.

	Distillation progress [°C]					
Compound	Start	10 %	50 %	90 %	95 %	End
(IAA)MM	126.3	127.7	130.4	132.8	134.0	142.3
D(IAA)M	199.2	202.6	203.2	203.7	204.2	207.1
(INA)MM	173.0	208.3	212.1	215.6	217.9	227.3
(INA)(IAA)M	234.4	238.3	249.4	262.8	264.4	266.1
D(INA)M	298.8	303.8	309.5	315.4	316.2	316.4

Fig. 9 demonstrates the correlation between molar mass and density of the considered compounds. The lowest values overall are registered for n-alkanes while an increment of density with increasing chain length can be observed. OMDME also showcase an increasing density with higher chain length, i.e., higher molar mass and also higher oxygen content in the backbone of the molecular structure. All OMDAE have a similar density in the range of 836–857 kg m^{-3}, which is very close to the value of 859 kg m^{-3} for DMM. OME in general exhibit higher densities when compared with n-alkanes with similar molar mass. This is most likely due to an overall higher oxygen content of OME, leading to stronger intermolecular forces and thus resulting in higher packing density. OMDME with a higher chain length feature a higher oxygen content than OMDAE with similar molar mass, indicating the effect of oxygen in regard to density.

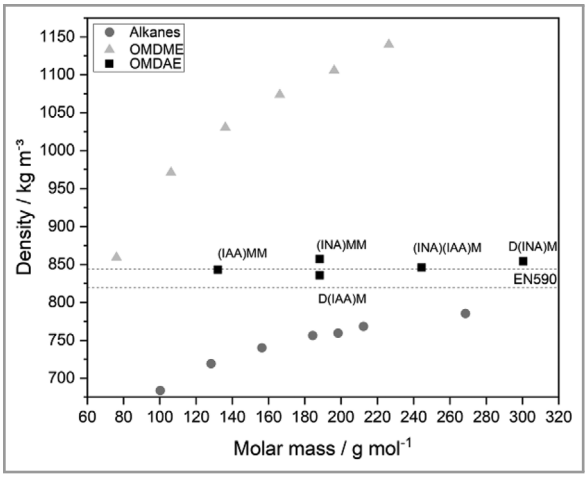

Figure 9. Densities of OMDAE in comparison with methanol-based OMDME, as well as *n*-alkanes with similar molar mass (values at 15 °C and atmospheric pressure).

The relationship between boiling characteristics and molar mass is depicted in Fig. 10. It is observed that a higher molar mass correlates with a higher boiling point, which can be explained by increased attractive intermolecular forces [52]. Branched molecules show smaller surface areas than isomers with straight chains, generally resulting in smaller attractive forces and therefore lower boiling points [35, 52]. This could explain the slightly lower boiling points of the branched OMDAE in comparison to the other considered substances.

The cold-stability of the studied compounds is displayed in Fig. 11. Due to measuring limits of the apparatus, the values of cold-stability properties for some compounds could not be determined. Here, the limit is marked with an arrow,

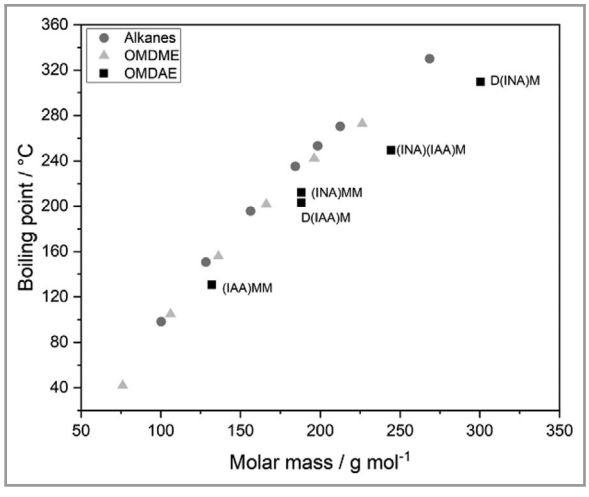

Figure 10. Boiling characteristics of OMDAE in comparison with methanol-based OMDME, as well as *n*-alkanes with similar molar mass (values at atmospheric pressure).

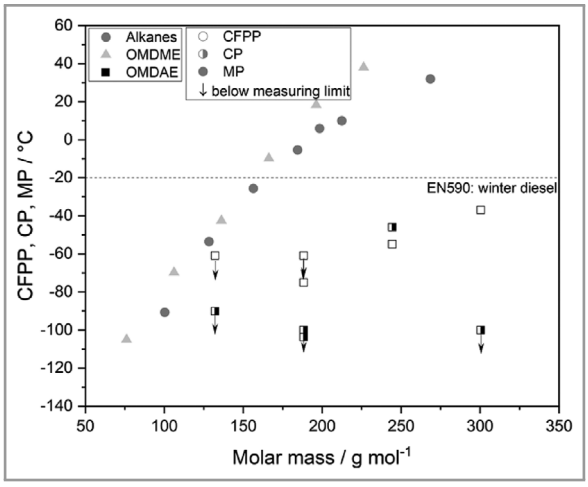

Figure 11. Cold-stability properties (CFPP = cold filter plugging point, CP = cloud point, MP = melting point) of OMDAE in comparison with methanol-based OME (OMDME), as well as *n*-alkanes with similar molar mass. The dashed line shows the upper limit for the CFPP according to the diesel standard EN 590. Empty symbols represent the CFPP value, half-filled symbols the CP value, and filled symbols the MP value (values at atmospheric pressure).

indicating that the actual value would be below the measuring limit. As expected for OMDME and *n*-alkanes, with increasing molar mass the melting point also rises due to higher attractive intermolecular forces [52]. In the case of the synthesized OMDAE, when compared to the compounds with similar molar mass, an improvement in the cold-stability properties can be seen, due to the branching effect of the present alkyl chains [35, 52]. Branching leads to steric hindrance, which in turn causes reduced packaging density. As a result, the molecules exhibit weaker attractive forces and are therefore less able to aggregate, thus increasing the cold-stability.

Regarding further fuel properties, the cetane number is of large importance. This property is useful to determine the ignition delay of the fuel and is an indication of the necessary compression for ignition in the engine chamber. The comparison between *n*-alkanes, OMDME, and OMDAE can be seen in Fig. 12. The EN 590 standard stipulates a cetane number above 51, and all the synthesized compounds meet this criterion.

In a study performed by Han et al. [53] it is described that branched alkanes and ethers show less favorable ignition properties than their linear counterparts. In general, the formation of radicals as well as their reaction with oxygen strongly influences the ignition delay of fuels. In branched molecules there are more primary carbons present, which in turn have higher bond-energy and therefore hinder the formation of transition rings necessary for fuel combustion. Also, the steric hindrance of branches decreases the probability of O atoms capturing targeted H atoms, a necessary process for fuel combustion [53]. In summary, longer alkyl

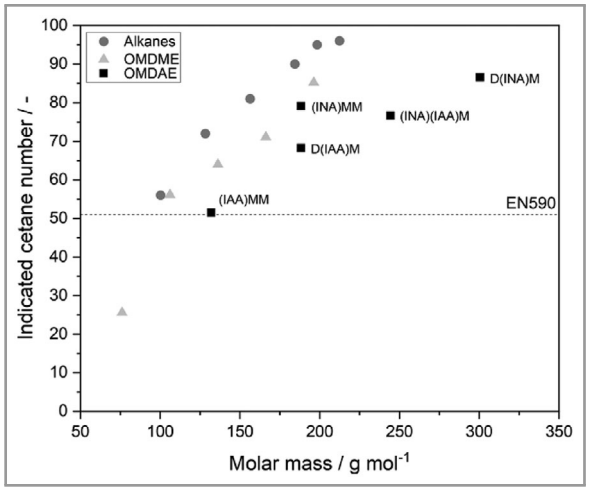

Figure 12. Cetane numbers of OMDAE in comparison with methanol-based OME (OMDME), as well as *n*-alkanes with similar molar mass. The dashed line shows the lower limit for the cetane number according to the diesel standard EN 590 (static pressure in the chamber before the test injections is 1.75 MPa, injection pressure is 100.0 MPa, and air temperature in the chamber is 580 °C).

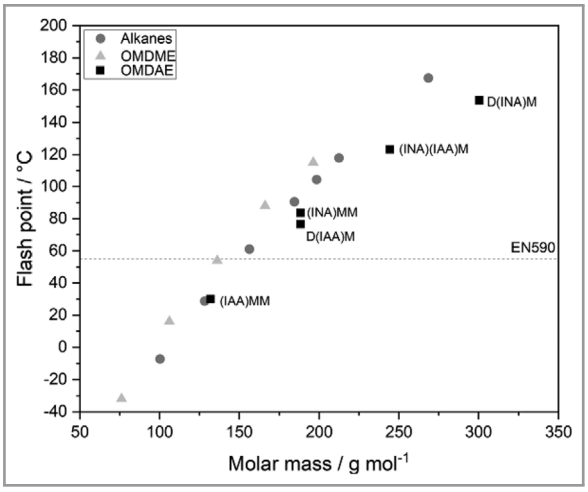

Figure 13. Flash points of OMDAE in comparison with methanol-based OME (OMDME), as well as *n*-alkanes with similar molar mass. The dashed line shows the lower limit for the flash point according to the diesel standard EN 590 (values at atmospheric pressure).

chains in the OME molecule lead to higher values for the cetane number (e.g., for D(INA)M), and branching causes a decrease of the cetane number (e.g., D(IAA)M compared to (INA)MM with the same molar mass).

The flash point (FP) is a safety parameter, playing an important role in the storage and transportation of materials in general. It indicates the lowest temperature at atmospheric pressure in which a flammable mixture of air and vapor is able to ignite in a closed environment. The relation between flash point and molar mass is demonstrated in Fig. 13. The flash point shows a strong correlation with the boiling point, which in turn indicates a strong relation to the molar mass of the compound, explaining higher flash points with increasing molar mass. As can be seen from Fig. 13, all considered substances with comparable molar mass show similar flash points. With exception of the lightest transacetal (IAA)MM, all synthesized compounds meet the criterion of the standard EN 590.

The lubricity of diesel fuels is indicated by the high frequency reciprocating rig (HFRR) value. This value is of due importance because moving parts of modern injection devices are lubricated by the fuel itself. The relation between lubricity and molar mass is depicted in Fig. 14. In regard to the OMDAE, only D(INA)M fulfills the criterion of the standard EN 590. Oxygen tends to enhance lubricity [54]. However, oxygenated functional groups have different effects on the lubricity of diesel fuels and ether groups (which would be the closest one to the acetal functional group) have one of the lowest enhancement effects on lubricity [54]. Generally, the thickness of the protecting film increases with the molecular chain length, thus an increment in chain length improves lubricity [54]. This would explain the lower HFRR value of D(INA)M (i.e., better lubricity), the compound featuring the longest alkyl chain as a symmetrical acetal.

In order to ensure optimal fuel injection, compliance with the viscosity specifications of the standard EN 590 is of key importance. The trend of viscosity with increasing molar mass is illustrated in Fig. 15. Due to higher attractive intermolecular forces, the viscosity rises with increasing molar mass. Only two of the synthesized OMDAE compounds, namely, (INA)(IAA)M and D(INA)M, are compatible with

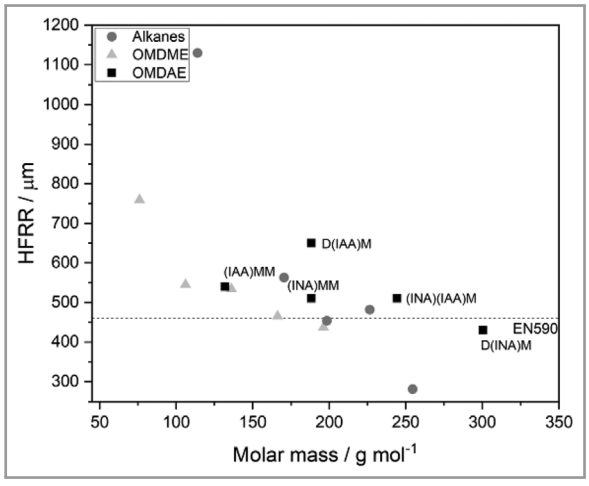

Figure 14. Lubricity (HFRR) of OMDAE in comparison with methanol-based OME (OMDME), as well as *n*-alkanes with similar molar mass. The dashed line shows the upper limit for the lubricity according to the diesel standard EN 590 (values at 60 °C and atmospheric pressure).

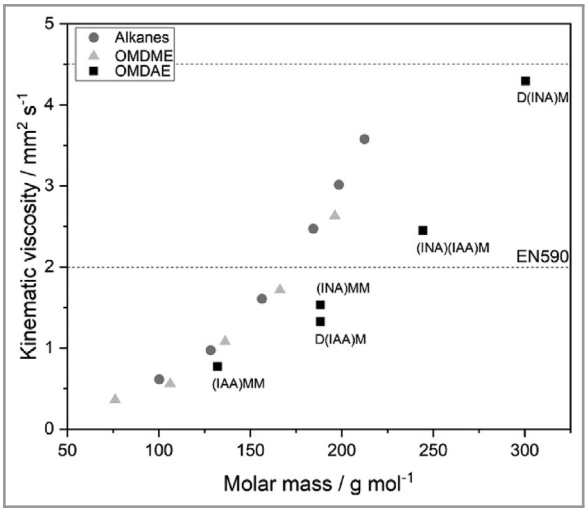

Figure 15. Kinematic viscosity of OMDAE in comparison with methanol-based OME (OMDME), as well as *n*-alkanes with similar molar mass. The dashed line shows the upper and lower limit for the kinematic viscosity according to the diesel standard EN 590 (values at 40 °C and atmospheric pressure).

the diesel standard. The considered OMDAE have a lower oxygen content than OMDME, thus the OMDAE showcase densities with lower packing and, therefore, lower viscosities. In addition, the steric hindrance of the branched molecules also leads to lower packing densities, i.e., lower values for viscosities.

In regard to the HHV, a linear fit with the oxygen content of the considered compounds can be observed in Fig. 16. A good correlation can be seen between these two variables. As expected, the higher the amount of longer alkyl chains, i.e., the lower the oxygen content, the higher the energy density in the molecule. The oxygen content of OMDME lies between 40 and 50 wt %, while the OMDAE synthesized in this work are in the range of 10 to 25 wt %.

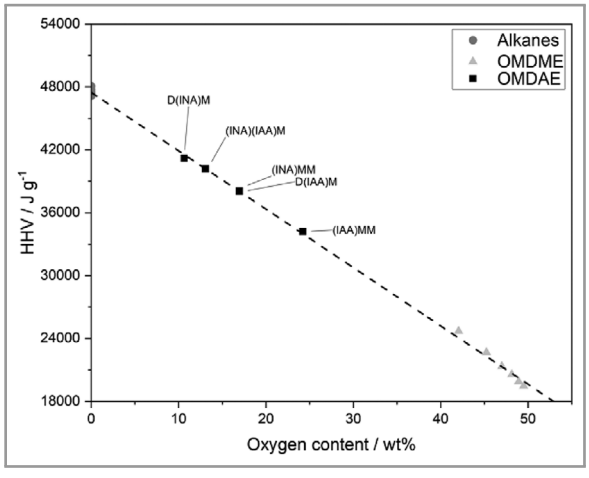

Figure 16. Correlation between higher heating value and oxygen content of OMDAE in comparison with methanol-based OME (OMDME), as well as *n*-alkanes with similar molar mass (values at 3 MPa pressure (bara)).

Considering the application as fuels, the synthesized OMDAE exhibit heating values between those of OMDME and *n*-alkanes. Having a lower HHV corresponds to a higher fuel consumption during combustion. For instance, the application of OMDME would translate in an increase of 70–80 vol. % of fuel injection when compared to conventional diesel [55]. Thus, engine adaptations would be required, such as larger injection nozzles and adjustment of engine control. As seen in the description of the relevant properties above, by employing different alcohols other than methanol in the OME synthesis it is possible to synthesize compounds with tailored properties according to the respective requirements. Previously, OMDME with a chain length of $n = 3$–5 have been intensively studied as alternative diesel fuels, since they exhibit the highest potential for soot reduction [32].

OMDAE based on technical alcohol mixtures and mixtures of isomers, such as IAA and INA, exhibit more compatible characteristics as diesel alternatives when compared to OMDME. Synthesis of modified OME could be integrated into OMDME synthesis by introducing alcohols other than methanol to the process. This would generate a distribution of OME with different chain lengths and different end groups, possibly enabling a mixture of oxygenates compliant with all requirements of the standard EN 590, especially if used as a blending component with conventional or paraffinic diesel.

3.3 Possible Applications

With the synthesis of modified OME, a high flexibility regarding applications emerges. A design of chemicals with desired properties becomes possible by employing the correct combination of alcohols or by using transacetalization reactions as a refining step. For instance, when comparing compounds with the same amount of oxymethylene repetition units, a higher flash point and a lower density can be achieved by using isoamyl alcohol, producing D(IAA)M, instead of using methanol, which would produce DMM.

The OMDAE based on isoamyl alcohol and isononyl alcohol show potential as blending components in diesel fuels since many properties are in accordance with the diesel standard EN 590, as can be seen from Tab. 3. A further application in the fuel sector could be as blending component with HVO, since combining the positive fuel properties of OME and HVO would result in a fuel blend with low emission profile as well as low carbon footprint [28]. A challenging aspect regarding the OME/HVO blend is guaranteeing the miscibility between the components, especially at lower temperatures [22–28].

In a simple qualitative study, a comparison of the miscibility of classical OMDME and OMDAE with HVO was

performed. To ensure comparability, all fuel samples were dried with calcium hydride prior to use. When using the synthesized OMDAE in the fuel blend, complete miscibility was observed both at room temperature and at −20 °C, regardless of the blend composition. When employing commercially available $OMDME_{3\text{-}5}$, a de-mixing with clear phase separation at room temperature was observed when 30 vol. % of $OMDME_{3\text{-}5}$ (70 vol. % of HVO) was used. At −20 °C, a solidification of the sample was observed with less than 5 vol. % $OMDME_{3\text{-}5}$ (>95 vol. % HVO).

As a follow-up, the commercially available $OMDME_{3\text{-}5}$ mixture was purified by distillation and a mixture of $OMDME_{3,4}$ was obtained (60 wt % $OMDME_3$ and 40 wt % $OMDME_4$). Here, it was observed that the fuel mixture only showed phase separation at higher percentages of OMDME. At room temperature, a de-mixing with clear phase separation was detected when 40 vol. % of $OMDME_{3,4}$ (60 vol. % of HVO) was used and at −20 °C when 9 vol. % of $OMDME_{3,4}$ (91 vol. % HVO) was employed, without formation of a solid phase in the sample container. This showcases that an adaptation of the OME molecular structure enhances the compatibility with paraffinic diesel. This can be achieved by employing shorter chain lengths of OMDME (e.g., only $OMDME_3$ and $OMDME_4$ mixtures) or by reducing the polarity of the OME molecule with longer alkyl end groups as in the case of OMDAE.

A further possibility to make use of the enhanced miscibility of OMDAE with longer alkyl end groups with HVO is to develop an extraction procedure to directly generate an OME/HVO fuel mixture. This was described by Oestreich et al. [23], who demonstrated a one-step synthesis and extraction procedure. *n*-Dodecane, diesel and HVO were used as extraction agents and extraction during synthesis of oxymethylene dimethyl ethers (OMDME) and oxymethylene diethyl ethers (OMDEE) was investigated. When utilizing *n*-dodecane, the total amount of OME in the organic phase amounted to 13 wt % for OMDME and 18 wt % for OMDEE, demonstrating an increased solubility in nonpolar media for the longer-chain OME. Similar values were achieved for the diesel fuels in the study.

In summary, the synthesized OMDAE based on C_5- and C_9-alcohols feature better solubility in nonpolar media when compared to OMDME, as can also be demonstrated by this qualitative study. Therefore, it would be possible to perform a modified OME synthesis by employing different alcohols and performing an extraction procedure with HVO afterwards, directly producing an OME/HVO fuel blend without the need of a further distillation to obtain the desired OME fraction.

4 Conclusion

OME can be modified on molecular scale by employing different alcohols other than methanol in the synthesis step, thus introducing new end groups into the molecule. Regarding OME production, synthesis of modified OME could be integrated into classical OMDME synthesis simply by introducing alternative alcohols to the process. A variety of different OME can be produced, enabling the synthesis of OME with customized properties, e.g., to enhance fuel properties.

The properties of OMDAE, i.e., modified OME, based on isoamyl alcohol and isononyl alcohol proved to be advantageous when compared to classical OMDME regarding their fuel characteristics. Here, favorable cold-stability properties and higher energy densities can be achieved, leading to an easier implementation into the existing fuel infrastructure. In literature, OME with modified alkyl end groups (ethyl-, propyl-, butyl-, isopropyl-, and isobutyl-terminated) showed better compatibility with sealing materials, such as fluoroelastomers and polyether ether ketone (PEEK) polymers. Following this trend, the synthesized OME in this study based on C_5- and C_9-alcohols should also exhibit an improved compatibility with sealing materials when compared to classic OMDME. This leads to a better compatibility in the fuel sector, not only as neat fuels, but also as a blending component with HVO, thus enabling a renewable fuel blend with strongly reduced emissions. The use of alcohols other than methanol in the production process could enable a market launch of OMDME and OMDAE as diesel fuel components.

Synthesis of such modified OME also gains relevance in the context of recent discussions regarding new application fields beyond the fuel sector. Further applicability of OMDAE as useful intermediates in the fine chemical sector, e.g., as solvents, plasticizers, or additives, could be studied. By utilizing the versatility of the OME synthesis with different alcohols as building blocks, a variety of end groups can be inserted into the OME molecule, allowing the design of tailored compounds with useful properties according to the specific requirements of relevant industry sectors.

Future work should include engine testing of different OMDME/OMDAE/HVO/diesel blends in order to evaluate the potential for the reduction of emissions. The study of a direct OME synthesis based on different alcohols, in addition to methanol, coupled with an extraction of the reaction mixture with HVO could be a valid process intensification to enable the market launch of OME as a blending component in diesel fuels.

Supporting Information

Supporting information for this article can be found under DOI: https://doi.org/10.1002/cite.202400159.

Acknowledgment

The authors gratefully acknowledge financial support from the Bundesministerium für Bildung und Forschung (BMBF)

within the NAMOSYN Project (FKZ 03SF0566K0). We also thank Evonik Operations GmbH for providing samples of isononyl alcohol (INA).

Open access funding enabled and organized by Projekt DEAL.

Abbreviations

CFPP	cold filter plugging point
CP	cloud point
DME	dimethyl ether
DMM	dimethoxymethane
FA	formaldehyde
FID	flame ionization detector
FP	flash point
GC	gas chromatography
HFRR	high-frequency reciprocating rig
HHV	higher heating value
HSQC	heteronuclear single quantum coherence
HVO	hydrogenated vegetable oils
IAA	isoamyl alcohol
INA	isononyl alcohol
MP	melting point
MS	mass spectrometry
m/*z*	mass-to-charge ratio
NMR	nuclear magnetic resonance
OMDAE	oxymethylene dialkyl ethers
OMDEE	oxymethylene diethyl ethers
OMDME	oxymethylene dimethyl ethers
OME	oxymethylene ethers
PEEK	polyether ether ketone
rpm	rotations per minute

References

[1] OPEC, 2013 World Oil Outlook **2013**.

[2] F. Leach, G. Kalghatgi, R. Stone, P. Miles, *Transp. Eng.* **2020**, *1*, 100005. DOI: https://doi.org/10.1016/j.treng.2020.100005

[3] "ExxonMobil Global Outlook: Our view to 2050," available at https://corporate.exxonmobil.com/sustainability-and-reports/global-outlook, **2024**.

[4] P. Jaramillo, S. Kahn Ribeiro, P. Newman, S. Dhar, O. E. Diemuodeke, T. Kajino, D. S. Lee, S. B. Nugroho, X. Ou, A. Hammer Strømman, J. Whitehead, 2022: Transport. In IPCC, 2022: Climate Change 2022: Mitigation of Climate Change. Contribution of Working Group III to the Sixth Assessment Report of the Intergovernmental Panel on Climate Change **2022**.

[5] L. Lautenschütz, D. Oestreich, P. Seidenspinner, U. Arnold, E. Dinjus, J. Sauer, *Fuel* **2016**, *173*, 129–137. DOI: https://doi.org/10.1016/j.fuel.2016.01.060

[6] P. Dworschak, V. Berger, M. Härtl, G. Wachtmeister, *SAE Tech. Pap.* **2020**, 2020-01-0805. DOI: https://doi.org/10.4271/2020-01-0805

[7] J. Fang, Y. Liu, K. Wang, H. R. Shah, S. Mu, X. Lang, J. Wang, *Fuel* **2021**, *290*, 119789. DOI: https://doi.org/10.1016/j.fuel.2020.119789

[8] A. García, A. Gil, J. Monsalve-Serrano, R. Lago Sari, *Fuel* **2020**, *275*, 117898. DOI: https://doi.org/10.1016/j.fuel.2020.117898

[9] A. Gómez, J. A. Soriano, O. Armas, *Fuel* **2016**, *184*, 536–543. DOI: https://doi.org/10.1016/j.fuel.2016.07.049

[10] A. Omari, B. Heuser, S. Pischinger, C. Rüdinger, *Appl. Energy* **2019**, *239*, 1242–1249. DOI: https://doi.org/10.1016/j.apenergy.2019.02.035

[11] L. Pellegrini, M. Marchionna, R. Patrini, C. Beatrice, N. Del Giacomo, C. Guido, *SAE Tech. Pap.* **2012**, 2012-01-1053. DOI: https://doi.org/10.4271/2012-01-1053

[12] J. Song, K. Cheenkachorn, J. Wang, J. Perez, A. L. Boehman, P. J. Young, F. J. Waller, *Energy Fuels* **2002**, *16* (*2*), 294–301. DOI: https://doi.org/10.1021/ef010167t

[13] J. Wang, F. Wu, J. Xiao, S. Shuai, *Fuel* **2009**, *88* (*10*), 2037–2045. DOI: https://doi.org/10.1016/j.fuel.2009.02.045

[14] C. K. Westbrook, W. J. Pitz, H. J. Curran, *J. Phys. Chem. A* **2006**, *110* (*21*), 6912–6922. DOI: https://doi.org/10.1021/jp056362g

[15] K. Hackbarth, P. Haltenort, U. Arnold, J. Sauer, *Chem. Ing. Tech.* **2018**, *90* (*10*), 1520–1528. DOI: https://doi.org/10.1002/cite.201800068

[16] D. Deutsch, D. Oestreich, L. Lautenschütz, P. Haltenort, U. Arnold, J. Sauer, *Chem. Ing. Tech.* **2017**, *89* (*4*), 486–489. DOI: https://doi.org/10.1002/cite.201600158

[17] X. Lü, J. Yang, W. Zhang, Z. Huang, *Energy Fuels* **2005**, *19* (*5*), 1879–1888. DOI: https://doi.org/10.1021/ef0500179

[18] S. Mohankumar, P. Senthilkumar, Renewable Sustainable Energy Rev. **2017**, *80*, 1227–1238. DOI: https://doi.org/10.1016/j.rser.2017.05.133

[19] B. Rajesh Kumar, S. Saravanan, B. Sethuramasamyraja, D. Rana, *Fuel* **2017**, *199*, 670–683. DOI: https://doi.org/10.1016/j.fuel.2017.03.041

[20] Y. R. Tan, M. L. Botero, Y. Sheng, J. A. H. Dreyer, R. Xu, W. Yang, M. Kraft, *Fuel* **2018**, *224*, 499–506. DOI: https://doi.org/10.1016/j.fuel.2018.03.051

[21] Y. R. Tan, M. Salamanca, J. Akroyd, M. Kraft, *Combust. Flame* **2022**, *243*, 111849. DOI: https://doi.org/10.1016/j.combustflame.2021.111849

[22] C. F. Breitkreuz, A. Holzer, T. Fuchs, M. Günthner, H. Hasse, *Fuel* **2023**, *338*, 127337. DOI: https://doi.org/10.1016/j.fuel.2022.127337

[23] D. Oestreich, L. Lautenschütz, U. Arnold, J. Sauer, *Fuel* **2018**, *214*, 39–44. DOI: https://doi.org/10.1016/j.fuel.2017.10.116

[24] Z. Yang, C. Ren, S. Jiang, Y. Xin, Y. Hu, Z. Liu, *Fuel* **2022**, *307*, 121797. DOI: https://doi.org/10.1016/j.fuel.2021.121797

[25] M. Yu, C. Chen, X. Jiang, *Fuel* **2022**, *323*, 124348. DOI: https://doi.org/10.1016/j.fuel.2022.124348

[26] A. Holzer, M. Guenthner, *SAE Tech. Pap.* **2021**, 2021-01-0556. DOI: https://doi.org/10.4271/2021-01-0556

[27] J. Preuß, K. Munch, I. Denbratt, *Fuel* **2021**, *303*, 121275. DOI: https://doi.org/10.1016/j.fuel.2021.121275

[28] A. Holzer, M. Günthner, P. Jung, *Automot. Engine Technol.* **2022**, *7* (*3–4*), 369–383. DOI: https://doi.org/10.1007/s41104-022-00122-8

[29] M. A. Arellano-Treviño, T. L. Alleman, R. Brim, A. T. To, J. Zhu, C. S. McEnally, C. Hays, J. Luecke, L. D. Pfefferle, T. D. Foust, D. A. Ruddy, *Fuel* **2022**, *322*, 124220. DOI: https://doi.org/10.1016/j.fuel.2022.124220

[30] G. An, Y. Xia, Z. Xue, H. Shang, S. Cui, C. Lu, *ACS Omega* **2022**, *7* (*3*), 3064–3072. DOI: https://doi.org/10.1021/acsomega.1c06452

[31] M. A. Arellano-Treviño, F. G. Baddour, A. T. To, T. L. Alleman, C. Hays, J. Luecke, J. Zhu, C. S. McEnally, L. D. Pfefferle, T. D. Foust, D. A. Ruddy, *Fuel* **2024**, *358*, 130353. DOI: https://doi.org/10.1016/j.fuel.2023.130353

[32] S. P. Lucas, F. L. Chan, G. M. Fioroni, T. D. Foust, A. Gilbert, J. Luecke, C. S. McEnally, J. J. A. Serdoncillo, A. J. Zdanowicz, J. Zhu, B. Windom, *Energy Fuels* **2022**, *36* (*17*), 10213–10225. DOI: https://doi.org/10.1021/acs.energyfuels.2c01414
[33] D. L. Bartholet, M. A. Arellano-Treviño, F. L. Chan, S. Lucas, J. Zhu, P. C. St John, T. L. Alleman, C. S. McEnally, L. D. Pfefferle, D. A. Ruddy, B. Windom, T. D. Foust, K. F. Reardon, *Fuel* **2021**, *295*, 120509. DOI: https://doi.org/10.1016/j.fuel.2021.120509
[34] M. A. Arellano-Treviño, D. Bartholet, A. T. To, A. W. Bartling, F. G. Baddour, T. L. Alleman, E. D. Christensen, G. M. Fioroni, C. Hays, J. Luecke, J. Zhu, C. S. McEnally, L. D. Pfefferle, K. F. Reardon, T. D. Foust, D. A. Ruddy, *ACS Sustainable Chem. Eng.* **2021**, *9* (*18*), 6266–6273. DOI: https://doi.org/10.1021/acssuschemeng.0c09216
[35] M. Drexler, P. Haltenort, T. A. Zevaco, U. Arnold, J. Sauer, *Sustainable Energy Fuels* **2021**, *5* (*17*), 4311–4326. DOI: https://doi.org/10.1039/D1SE00631B
[36] P. Haltenort, L. Lautenschütz, U. Arnold, J. Sauer, *Top. Catal.* **2019**, *62* (*5–6*), 551–559. DOI: https://doi.org/10.1007/s11244-019-01188-9
[37] P. Haltenort, K. Hackbarth, D. Oestreich, L. Lautenschütz, U. Arnold, J. Sauer, *Catal. Commun.* **2018**, *109*, 80–84. DOI: https://doi.org/10.1016/j.catcom.2018.02.013
[38] J. Voggenreiter, P. Van De Zande, J. Burger, *Chem. Eng. Sci.* **2022**, *262*, 117995. DOI: https://doi.org/10.1016/j.ces.2022.117995
[39] M. A. Tike, V. V. Mahajani, *Can. J. Chem. Eng.* **2008**, *84* (*4*), 452–458. DOI: https://doi.org/10.1002/cjce.5450840406
[40] "Isononanol (INA) - Evonik Industries," available at https://c4-chemicals.evonik.com/en/Products/isononanol-ina-167924.html, **2024**.
[41] C. Fuchs, U. Arnold, J. Sauer, *Chem. Ing. Tech.* **2023**, *95* (*5*), 651–657. DOI: https://doi.org/10.1002/cite.202200209
[42] S. Rodgers, F. Meng, S. Poulston, A. Conradie, J. McKechnie, *J. Cleaner Prod.* **2022**, *364*, 132614. DOI: https://doi.org/10.1016/j.jclepro.2022.132614
[43] M. Beller, *Catalytic Carbonylation Reactions*, Vol. *18*, Springer, Berlin **2006**.
[44] C. J. Baranowski, T. Fovanna, M. Roger, M. Signorile, J. McCaig, A. M. Bahmanpour, D. Ferri, O. Kröcher, *ACS Catal.* **2020**, *10* (*15*), 8106–8119. DOI: https://doi.org/10.1021/acscatal.0c01805
[45] M. Ouda, G. Yarce, R. J. White, M. Hadrich, D. Himmel, A. Schaadt, H. Klein, E. Jacob, I. Krossing, *React. Chem. Eng.* **2017**, *2* (*1*), 50–59. DOI: https://doi.org/10.1039/C6RE00145A
[46] M. Drexler, P. Haltenort, U. Arnold, J. Sauer, *Chem. Ing. Tech.* **2022**, *94* (*3*), 256–266. DOI: https://doi.org/10.1002/cite.202100173
[47] Atlas of Zeolite Framework Types, 5th ed. (Eds.: C. Baerlocher, W. M. Meier, D. H. Olson), Elsevier, Amsterdam **2001**.
[48] E. Müller, O. Bayer, H. Meerwein, K. Ziegler, *in Methoden der Organischen Chemie (Houben-Weyl)*, Georg Thieme Verlag, Stuttgart **1954**.
[49] J. Guilera, E. Ramírez, C. Fité, M. Iborra, J. Tejero, *Appl. Catal., A* **2013**, *467*, 301–309. DOI: https://doi.org/10.1016/j.apcata.2013.07.024
[50] N. G. Polyanskii, P. E. Tulupov, *Russ. Chem. Rev.* **1971**, *40* (*12*), 1030–1046. DOI: https://doi.org/10.1070/RC1971v040n12ABEH001990
[51] K. A. Sheikh, V. Zaghini Francesconi, T. A. Zevaco, J. Sauer, *Catal. Sci. Technol.* **2024**, *14* (*5*), 1148–1166. DOI: https://doi.org/10.1039/D3CY01286G
[52] *Organic Chemistry: Structure and Function*, 8th ed. (Eds.: P. Vollhardt, N. Schore), W.H. Freeman and Company, New York **2018**.
[53] W.-Q. Han, C.-D. Yao, *Fuel* **2015**, *150*, 29–40. DOI: https://doi.org/10.1016/j.fuel.2015.01.090
[54] E. Sukjit, P. Poapongsakorn, K. D. Dearn, M. Lapuerta, J. Sánchez-Valdepeñas, *Wear* **2017**, *376–377*, 836–842. DOI: https://doi.org/10.1016/j.wear.2017.02.007
[55] *11. Tagung Einspritzung und Kraftstoffe 2018: Diesel · Benzin · Gas · Alternative Kraftstoffe · Medien für SCR · Wasser* (Eds.: H. Tschöke, R. Marohn), Springer Fachmedien, Wiesbaden **2019**.

